ACS APPLIED BIO MATERIALS

www.acsabm.org Article

Antifouling Coatings Generated from Unsymmetrical Partially Fluorinated Spiroalkanedithiols

Lydia R. St. Hill, John W. Craft, Jr, Pawilai Chinwangso, Hung-Vu Tran, Maria D. Marquez, and T. Randall Lee*

Cite This: *ACS Appl. Bio Mater.* 2021, 4, 1563−1572 Read Online

ACCESS | Metrics & More | Article Recommendations | Supporting Information

ABSTRACT: Biofouling negatively impacts modern society on a daily basis, especially with regard to the important industries of medicine, oil, and shipping. This manuscript describes the preparation and study of model antifouling coatings generated from the adsorption of unsymmetrical partially fluorinated spiroalkanedithiols on gold. The antifouling properties of the self-assembled monolayers (SAMs) derived from the spiroalkanedithiols were compared to SAMs derived from analogous monodentate partially fluorinated and nonfluorinated alkanethiols.

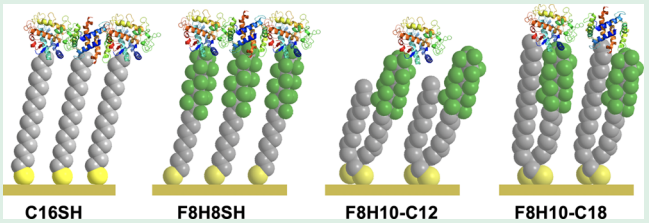

The antifouling properties were evaluated using *in situ* surface plasmon resonance spectroscopy (SPR), *ex situ* electrochemical quartz crystal microbalance (QCM) measurements, and *ex situ* ellipsometric thickness measurements. The resistance to nonspecific protein adsorption of the SAMs was evaluated with proteins having a wide range of properties and applications including protamine, lysozyme, bovine serum albumin, and fibrinogen. The results from the SPR and the QCM measurements demonstrated that in most cases, the SAM coatings derived from the partially fluorinated spiroalkanedithiols having mixed hydrocarbon and fluorocarbon tail groups exhibited better antifouling performance when compared to the SAMs derived from their single-component monodentate counterparts. The studies also revealed that while the SPR and the QCM measurements in most cases were able to distinguish the adsorption trends for the SAMs and proteins examined, the ellipsometric thickness measurements were markedly less discriminating. On the whole, these studies validate the use of unsymmetrical partially fluorinated spiroalkanedithiols for generating effective antifouling coatings on metal substrates.

KEYWORDS: *antifouling, self-assembled monolayers, fluorinated, spiroalkanedithiols, surface plasmon resonance, quartz crystal microbalance, ellipsometry*

INTRODUCTION

Biofouling or biocontamination creates challenges in various applications, including biosensors, medical implants, surgical instruments, marine equipment, cookware, protective apparel, and food packaging.[1−3] In medical devices, biocontamination can interfere with device performance, product efficiency, and customer safety.[2,4,5] Moreover, uncontrolled adhesion of biomaterials (*e.g.*, proteins) on implanted medical devices can diminish the effectiveness of the device and affect the patient's health.[2,4] Consequently, research on novel antifouling coatings remains an active area of research in materials and interfacial science.[1−3,6−10] To this end, organic thin films bearing polyethylene glycol (PEG) termini have been widely used as coatings for biomedical applications.[11] While exhibiting a high degree of biological inertness,[12] PEG-based coatings suffer from the reactivity of the PEG molecules toward hydration at high temperatures, as well as oxidation by atmospheric oxygen in the presence of transitional metal ions.[6,13−15] Ubiquitous polytetrafluoroethylene (PTFE), commonly known as Teflon, is an alternative antiadhesive material whose repeat units have been incorporated into thin-film coatings.[16−18] PTFE-based films are well-recognized antiadhesive materials with desirable interfacial properties, such as low wettability, low friction, and low adhesion.[2,19−21] Consequently, the introduction of fluorocarbon segments in nanostructured thin films (1−2 nm thickness) can lead to materials with unique interfacial properties that limit the biofouling of surfaces.

Thin-film coatings generated using the process of self-assembly afford well-defined, highly ordered surfaces known as self-assembled monolayers (SAMs).[22−24] A wide variety of SAMs with distinct interfacial properties have been generated from systematically designed adsorbates for use in targeted applications as well as fundamental studies of interfacial science.[25−27] SAMs generated by the adsorption of thiols on

Received: October 29, 2020
Accepted: January 14, 2021
Published: February 1, 2021

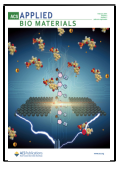

https://dx.doi.org/10.1021/acsabm.0c01409
ACS Appl. Bio Mater. 2021, 4, 1563−1572

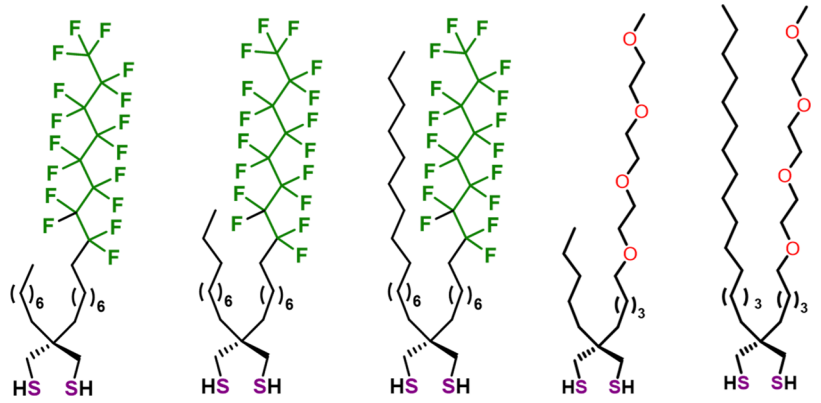

Figure 1. Unsymmetrical spiroalkanedithiols (SADTs) bearing two chemically dissimilar chains.[39,50−52]

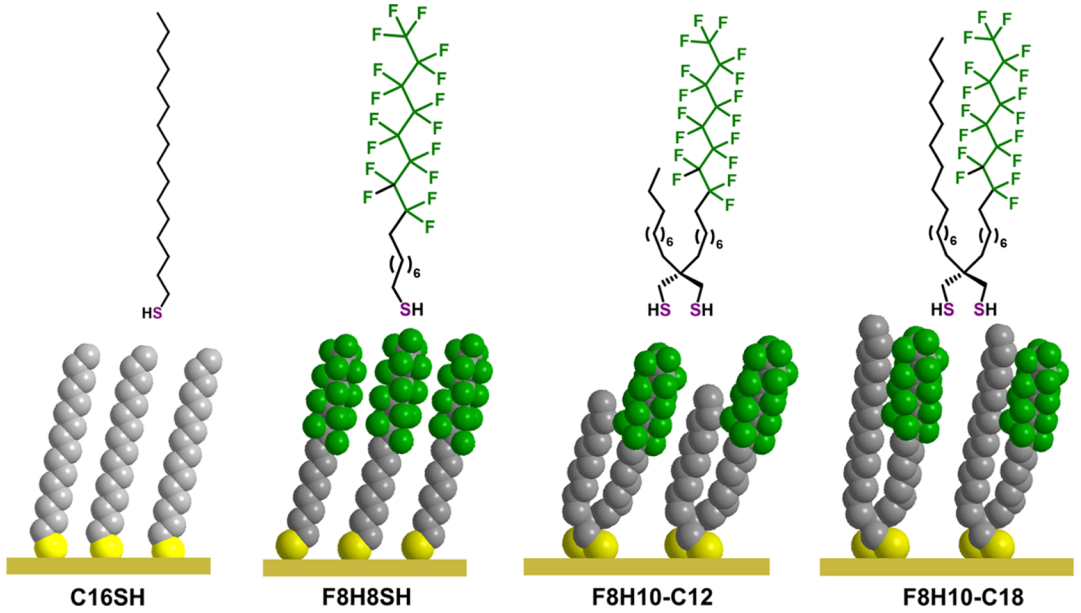

Figure 2. Adsorbate structures used to generate SAMs in this study: monodentate **C16SH** and **F8H8SH** (left) and bidentate **F8H10-C12** and **F8H10-C18** (right).

gold surfaces serve as a particularly versatile system for studying the interfacial properties of films, offering unprecedented insights into the development of effective antifouling surfaces.[15,28−34] SAMs on gold enjoy several advantages including high reproducibility, wide functional group tolerance, and interfacial tunability *via* the use of adsorbates bearing selected tail groups.[12,15,16,28] Well-established chemical reactions have been used to synthesize adsorbates bearing PEG, charged, or zwitterionic tail groups for generating a variety of antifouling surfaces.[25,29−34] Furthermore, these tools have allowed for the synthesis of partially fluorinated adsorbates to generate thin films with interfacial properties similar to those of PTFE. Thus, similar to PTFE, fluorinated SAMs (FSAMs) have been shown to exhibit high hydrophobic and oleophobic behavior, as well as chemical and thermal stability.[2,16,35−37] The incorporation of fluorinated termini in the structure of thiol-based adsorbates bridges the gaps in applications where the use of fluorinated polymers is inappropriate. Research on fluorinated SAMs has shown that the structure of the film is greatly affected by the hydrocarbon spacer of the adsorbates, whereas the fluorinated segments dictate the interfacial properties and thermal stability of the film.[16−18,35−37]

An emerging method for tuning the interfacial properties of thin-film coatings is the use of mixed adsorbates bearing dissimilar functional groups to generate unique nanoscale interfaces composed of phase-incompatible chemical entities.[30,38−40,45] However, the incorporation of two different monodentate thiols possessing chemically dissimilar tail groups often leads to films comprised of phase-separated domains due to their incompatibility.[41−44] Only recently, Chinwangso and co-workers demonstrated the ability to generate films with controlled interfacial heterogeneity by linking two chemically dissimilar chains—a hydrocarbon chain with a partially fluorinated chain or an oligo(ethylene glycol) chain—on a bidentate spiroalkanedithiol (SADT) head group, as illustrated in Figure 1.[30,38−40,45]

Inspired by the unique antiadhesive properties as well as chemical and thermal stability of fluorinated SAMs and spiroalkanedithiol-based SAMs,[26,27,30,36] this manuscript describes the interactions between several common contaminant proteins and compositionally mixed interfaces generated from partially fluorinated spiroalkanedithiols. The overarching goal of this work is to generate interfacially "conflicted" monolayers on gold surfaces that resist protein adhesion. We use the term

https://dx.doi.org/10.1021/acsabm.0c01409
ACS Appl. Bio Mater. 2021, 4, 1563−1572

Table 1. Physical Properties of the Proteins Examined in This Investigation

protein	protamine[46]	lysozyme[47]	BSA[48]	fibrinogen[49,50]
molecular weight	4 KDa	14 KDa	55 KDa	340 KDa
shape	spherical	stubby prolate ellipsoid	prolate ellipsoid[a]	cylindrical[b]
size	5 Å[c]	18 Å[c]	140 × 40 × 40 Å	450 × 90 Å
pI	12.1	11.1	4.8	5.7
application	insulin	cell	blood	muscle/tissue

[a]Where $a = b < c$. [b]With round ends. [c]Diameter.

"conflicted" to emphasize that the interfaces are comprised of chemically disparate species that are held in close proximity while preferring to be phase-separated. Specifically, we generated SAMs from unsymmetrical partially fluorinated spiroalkanedithiols (SADTs), **F8H10-C12** and **F8H10-C18** (see Figure 2), to study protein adhesion on these unique compositionally heterogeneous surfaces. The performance of the partially fluorinated SADT-based SAMs was compared to SAMs generated from the analogous monodentate adsorbates *n*-alkanethiol **C16SH** and partially fluorinated alkanethiol **F8H8SH** to evaluate the effect of the adsorbate structure on the antiadhesive properties of the films. Given their wide range of sizes, structures, and chemical compositions, we chose protamine, lysozyme, bovine serum albumin (BSA), and fibrinogen to serve as model proteins to evaluate the antiadhesive properties of the "conflicted" interfaces.

We hypothesize that the chemical heterogeneity introduced at the interfaces of the bis-functionalized spiroalkanedithiol SAMs can plausibly lead to a reduction in favorable interactions between the contacting proteins and the surfaces as the SAMs are composed of disparate low-energy species.[38] We also expect that the perfluorinated segment will help maintain the structural integrity and increase the thermal stability of the films.[2,16,35−37] Notably, adsorbate **F8H8-C12** is designed to create SAMs that allow the bulky helical fluorinated segments to pack atop the underlying well-packed trans-extended alkyl chains.[40] We characterized the protein-resistant properties of the single-component and mixed SAMs by surface plasmon resonance (SPR), electrochemical quartz crystal microbalance (QCM), and ellipsometry. We anticipate that studies of these model SAM interfaces will guide the development of "conflicted" films as nanoscale antiadhesive coatings that can be fine-tuned to enhance the biocompatibility of medical implants and devices but also in the ever-important oil and shipping industries.

EXPERIMENTAL SECTION

The Supporting Information provides details regarding the materials, instrumentation, and procedures used to conduct the research in this manuscript (including details used to collect the SPR and QCM data). The adsorbates and SAMs utilized in the present study were fully characterized in previous reports.[39,40]

RESULTS AND DISCUSSION

We first established an initial, but not exhaustive, selection of testing environments to evaluate antifouling properties of the SAMs by examining proteins with a wide range of properties and applications. Proteins evaluated in this study were selected based on criteria including isoelectric point, size, molecular weight, hydrophobicity, and applications. Table 1 provides a description of the properties of the selected proteins. The set of proteins includes protamine, which was selected due to its applications in medicine and tissue engineering;[46] lysozyme, a small and positively charged protein;[47] BSA, a widely used, stable, and hydrophobic protein;[48] and fibrinogen, a widely used large and sticky protein.[49,50] All protein solutions were prepared by dissolving the protein in phosphate buffer solution (PBS) since it is well-tolerated by the selected proteins. Furthermore, to remove any anomalies in protein adhesion that might be caused by the buffer system,[51,52] we measured changes associated with the buffer exposed on each respective film and used this information as a reference for the protein experiments. We studied the nonspecific adsorption of the selected proteins on the surfaces of SAMs generated from unsymmetrical partially fluorinated spiroalkanedithiols (SADTs), **F8H10-C12** and **F8H10-C18**, along with monothiolate SAMs formed from a normal monodentate *n*-alkanethiol **C16SH** and a partially fluorinated alkanethiol **F8H8SH**. Such comparisons allow detailed structure−property relationships of the interfacially "conflicted" monolayers toward antifouling. Moreover, we also measured qualitatively both the surface coverage and the amount of protein on the SAM surfaces using surface plasmon resonance (SPR), electrochemical quartz crystal microbalance (QCM), and ellipsometry.

Together with ellipsometry,[30] a common and easily accessible method, we chose to explore the use of other, more sensitive biophysical techniques, such as SPR[53−55] and QCM,[56−59] to examine the protein resistance of thin films derived from the adsorbates, as shown in Figure 2. The biophysical methods are needed not only to evaluate the validity of the ellipsometry data but also to gain broader insight into the antifouling performance of the unique "conflicted" interfaces prepared herein. Importantly, both QCM and SPR provide data that are highly correlated to mass absorbance on the surfaces; consequently, we report in Figure 3 the adsorption behavior of four different proteins on the SAMs as determined by data obtained from SPR, QCM, and ellipsometry.

Before describing the results of each type of measurement (SPR, QCM, and ellipsometry) in detail, we note that the antifouling trends were most consistently demonstrated by the adsorption of the largest-molecular-weight protein fibrinogen (340 KDa) across all of the SAMs, where an overall picture emerged that the SAMs derived from the unsymmetrical partially fluorinated spiroalkanedithiol adsorbates were able to reduce the nonspecific absorption of fibrinogen. Specifically, the SPR values for fibrinogen on the **C16SH** and **F8H8SH** SAMs were 2531 ΔRU and 2533 ΔRU, respectively, which trended downward to 2327 ΔRU and 2344 ΔRU on the **F8H10-C18** and **F8H10-C12** SAMs, respectively (Figure 3A). Likewise, the QCM data showed large values of increased mass upon fibrinogen exposure, 792 and 793 ng/cm^2 for the **C16SH** and **F8H8SH** SAMs, respectively, which trended downward to 565 and 571 ng/cm^2 for the **F8H10-C18** and **F8H10-C12** SAMs, respectively (Figure 3B). These observations were

https://dx.doi.org/10.1021/acsabm.0c01409
ACS Appl. Bio Mater. 2021, 4, 1563−1572

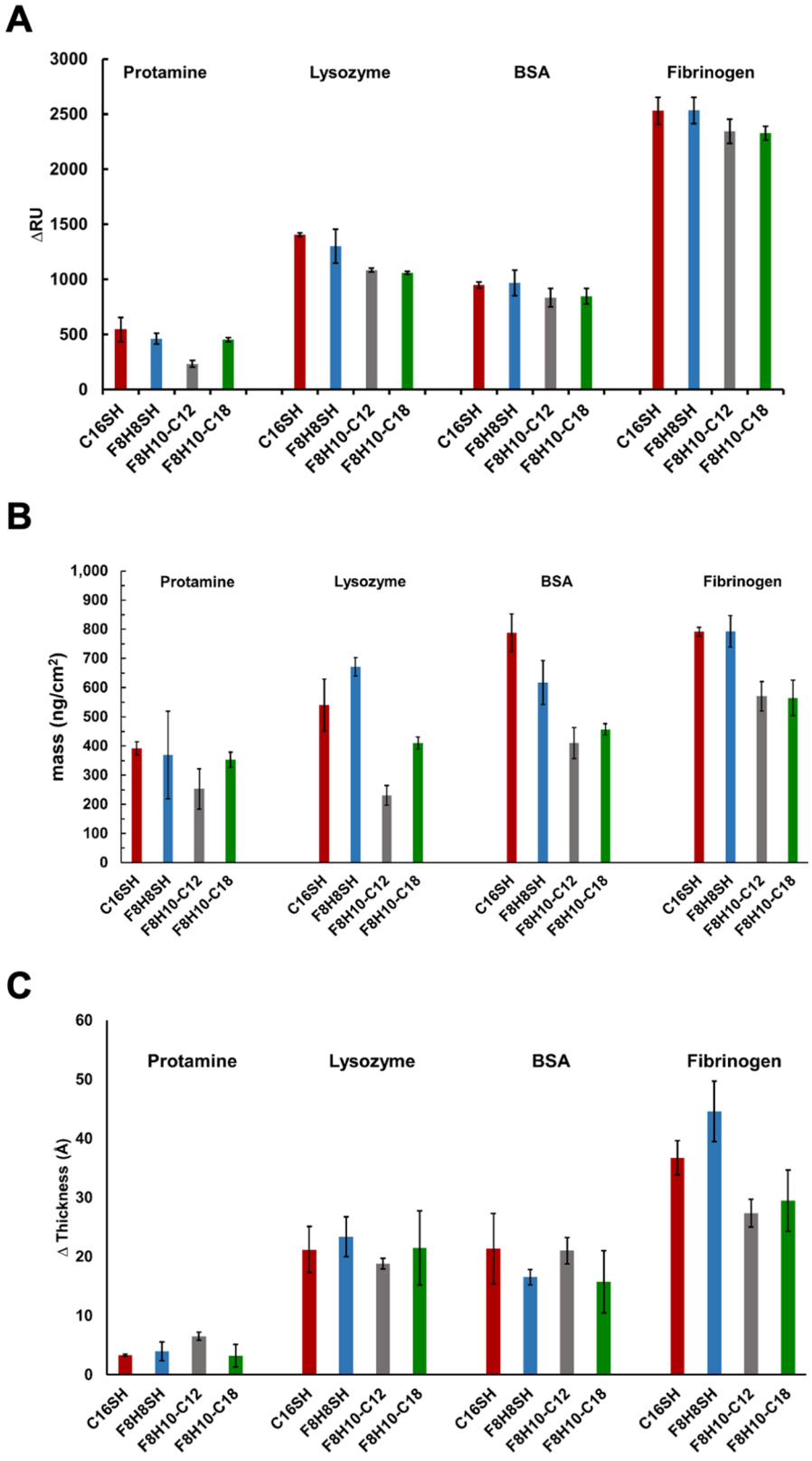

Figure 3. Inferred changes in mass/thickness for SAMs generated from **C16SH**, **F8H8SH**, **F8H10-C12**, and **F8H10-C18** upon exposure to solutions of protamine, lysozyme, BSA, and fibrinogen as measured by (A) SPR, (B) QCM, and (C) ellipsometry. The error bars were generated from measurements on three independent samples of each surface and protein.

corroborated by the ellipsometry data (Figure 3C), where the greatest increases in thickness were 37 and 45 Å for the **C16SH** and **F8H8SH** SAMs, respectively, compared to 27 and 30 Å for the **F8H10-C12** and **F8H10-C18** SAMs, respectively.

***In Situ* Analysis of Protein Adhesion Using SPR Spectroscopy.** Surface plasmon resonance (SPR) spectroscopy is a convenient technique to monitor the real-time *in situ* interaction of proteins with surfaces in both academic and

https://dx.doi.org/10.1021/acsabm.0c01409
ACS Appl. Bio Mater. 2021, 4, 1563−1572

industrial laboratories.[15,53] SPR is an optical technique that detects changes in the refractive index as the material adheres to a surface. Here, changes in response units are correlated to the amount of nonspecific proteins that adsorb on SAMs. Increasing material deposition generates increasingly large changes in response units (ΔRU). Figure 4 displays sensorgrams reporting the response changes for the interactions between four selected proteins and the SAMs, while Table 2 shows the numerically calculated ΔRU values.

The SPR data in Figure 4 and Table 2 show generally that the SAMs derived from **C16SH** and **F8H8SH** absorbed larger amounts of proteins compared to the SAMs derived from **F8H10-C12** and **F8H10-C18**, particularly for the **F8H10-C12** SAMs. For example, protamine exposure produced ΔRU values of 544, 461, 233, and 453 for SAMs generated from **C16SH**, **F8H8SH**, **F8H10-C12**, and **F8H10-C18**, respectively. The value of ΔRU correlates to the amount of material interacting and binding to the surface of the SAM attached to the gold substrate. More protein binding on the surface would generate a greater response signal. Thus, a decrease in response units is expected with respect to the decrease in the amount of proteins on the surface. The data for protamine correspond to 15, 48, and 17% less protein adsorption on the surface of SAMs generated from **F8H8SH**, **F8H10-C12**, and **F8H10-C18**, respectively, compared to the **C16SH** SAMs (normalized at 100% protein adsorption). In this case, the **F8H10-C12** SAMs exhibited greater protein resistance than those generated from analogous **F8H10-C18**. Interestingly, when comparing the ΔRU values in Table 2 for the bidentate **F8H10-C12** and **F8H10-C18** SAMs upon exposure to lysozyme, BSA, and fibrinogen, these two SAMs showed no substantial differences in antifouling behavior; however, their ΔRU values were notably smaller than those found for the monodentate **C16SH** and **F8H8SH** SAMs.

Overall, the SAMs generated from the bidentate adsorbates (**F8H10-C12** and **F8H10-C18**) exhibited greater protein resistance than the SAMs generated from the monodentate analogues (**C16SH** and **F8H8SH**). Due, at least in part, to its hydrophobic nature (see Table 3), the **C16SH** SAM can interact strongly with hydrophobic patches on the proteins to afford large ΔRU values.[60] Compared to alkanethiol SAMs, fluorinated surfaces exhibit even greater hydrophobicity and lower surface energies.[20] The hydrophobicity and low surface energy of the fluorinated surface give rise to unfavorable interactions with the proteins (*i.e.*, repulsive interactions) when compared to the **C16SH** SAM. Specifically, for the **F8H8SH** SAM, the perfluorinated portion produces a hydrophobic surface with lower surface energy than alkanethiol SAMs.[35] In the case of the **F8H10-C12** SAM, greater protein resistance is likely due to the ability of the hydrophobic helical **F8** fluorinated chains (van der Waals diameter of ~5.6 Å) to extend above the underlying well-packed trans-extended alkyl chains (van der Waals diameter ~4.2 Å).[61−63] Specifically, inclusion of the **C12** alkyl chains in the **F8H10-C12** SAM architecture allows the **F8** fluorinated chains to be more loosely packed than those in the corresponding monodentate SAM (**F8H8SH**),[40] thereby exposing greater numbers of antiadhesive interfacial CF_2 groups per unit area than in the **F8H8SH** SAMs.

In contrast to the **F8H10-C12** SAMs, the longer hydrocarbon chains in the **F8H10-C18** SAMs were found in previous studies to be detrimental to film order;[39,40] this phenomenon was attributed to unfavorable interactions between the two phase-incompatible groups that led to loosely packed chains exposing both CH_2 and CF_2 groups. Nevertheless, the SAMs derived from bidentate **F8H10-C18** were, on the whole, more protein-resistant than the SAMs derived from the monodentate analogues. Consequently, we attribute the enhanced protein resistance of the **F8H10-C18** SAMs to the heterogeneous mixture of interfacial hydrocarbon and

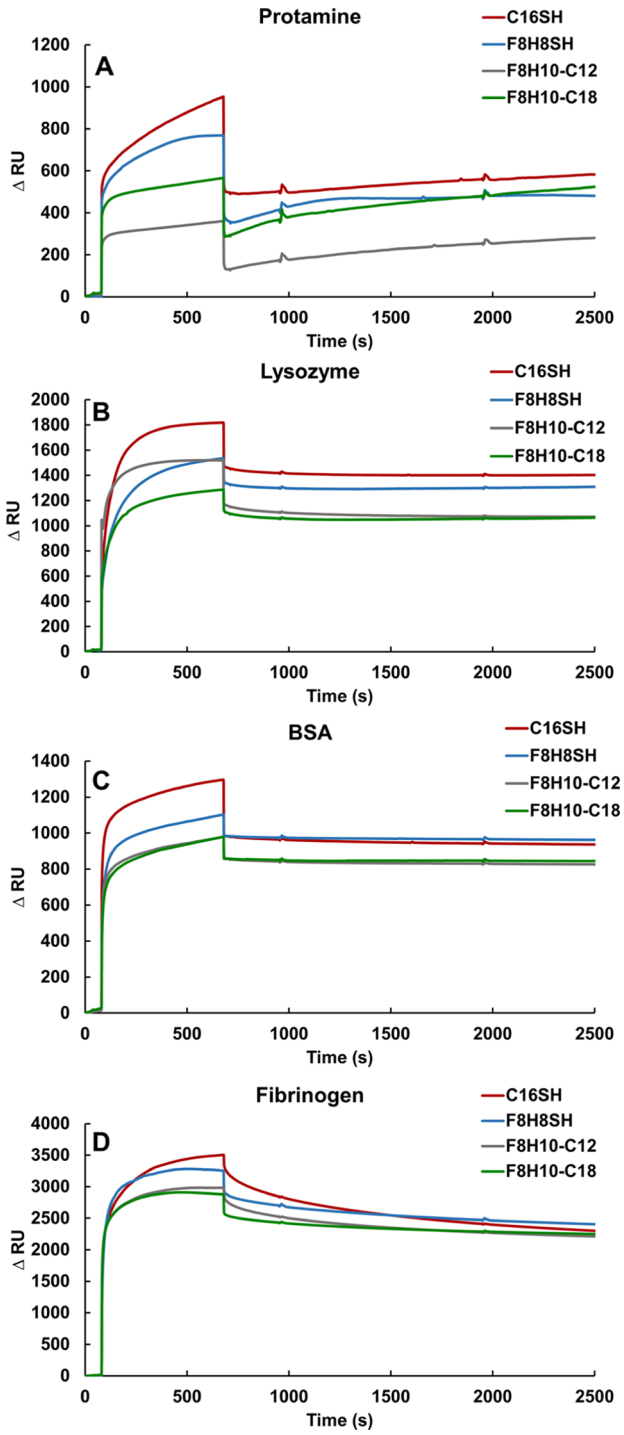

Figure 4. SPR sensorgrams of the SAMs exposed to (A) protamine, (B) lysozyme, (C) BSA, and (D) fibrinogen. Protein solutions were prepared at a concentration of 1 mg/mL in a PBS. The measurements were performed on three independent samples of each surface and protein with all trends consistent with those shown here.

https://dx.doi.org/10.1021/acsabm.0c01409
ACS Appl. Bio Mater. 2021, 4, 1563−1572

Table 2. ΔRU for SAMs after Exposure to Protein Solutions

adsorbate	protamine ΔRU	lysozyme ΔRU	BSA ΔRU	fibrinogen ΔRU
C16SH	544 ± 110	1407 ± 16	948 ± 28	2531 ± 122
F8H8SH	461 ± 49	1302 ± 153	968 ± 116	2533 ± 119
F8H10-C12	233 ± 30	1084 ± 18	833 ± 84	2344 ± 110
F8H10-C18	453 ± 19	1059 ± 14	847 ± 69	2327 ± 63

Table 3. Advancing Contact Angles (θa, ∘) for Water and Hexadecane as Probing Liquids on the SAM Surface

	water (H_2O) θa, ∘	hexadecane (HD) θa, ∘
C16SH	108	51
F8H8SH	120	83
F8H10-C12	125	73
F8H10-C18	121	59

fluorocarbon species, which represent an unnatural composition that is not found in nature.

Importantly, there is no convincing evidence that the size/molecular weight of the proteins has an influence on the ΔRU values; furthermore, the net charge of the proteins also seems to play no role on the amounts of protein adsorbed on the SAM surfaces. Similarly, there is no clear correlation with the surface energies of the SAMs: **C16SH** SAM (20.3 mJ/m^2), **F8H8SH** SAM (8.9 mJ/m^2), **F8H10-C12** SAM (11.5 mJ/m^2), and **F8H10-C18** SAM (15.8 mJ/m^2). Details of the surface energy calculations for the SAMs can be found in the Supporting Information (see Tables S2−S4). Given these observations, it is likely that, when comparing the respective proteins, the relative ΔRU values on these uniformly low-energy SAM surfaces are predominantly influenced by the sticky nature of the respective proteins, with the stickiest protein of all (fibrinogen),[49,50] showing the largest ΔRU values.

***Ex Situ* Analysis of Protein Adhesion Using QCM.** Taking advantage of the mass sensitivity of QCM sensors,[47,48,64,65] we also used QCM to quantify the amount of protein adhered to the SAM surfaces. Figure 5 shows the frequency change Δf as a function of time for all four SAM surfaces after 1 h exposure to 1 mg/mL of proteins in PBS; a decrease in frequency compared to the bare QCM sensor indicates the mass adsorbed onto the surface. The corresponding mass loadings of each protein on the surfaces (calculated using the Sauerbrey equation) are listed in Table 4. Each reported value is an average of three independent experiments. Notably, the data show greater mass changes after exposing protein solutions to the **C16SH** and **F8H8SH** SAMs compared to the **F8H10-C12** and **F8H10-C18** SAMs, indicating a lesser mass loading on the two bidentate SAMs. The QCM studies were conducted *ex situ* and therefore generated responses known as dry mass loading of proteins on the surface without the hydration layer, which should plausibly reflect lower protein loadings when compared to the data obtained from *in situ* measurements by SPR.[66−69] Nevertheless, similar trends would be expected from both methods.

As noted when analyzing the SPR data, the enhanced protein resistance observed by QCM for the **F8H10-C12** SAMs can be attributed to the extension of the hydrophobic helical **F8** fluorinated chains above the underlying densely packed alkyl chains, thereby exposing greater numbers of antiadhesive interfacial CF_2 groups per unit area than in the **F8H8SH** SAMs. Similarly, the enhanced protein resistance

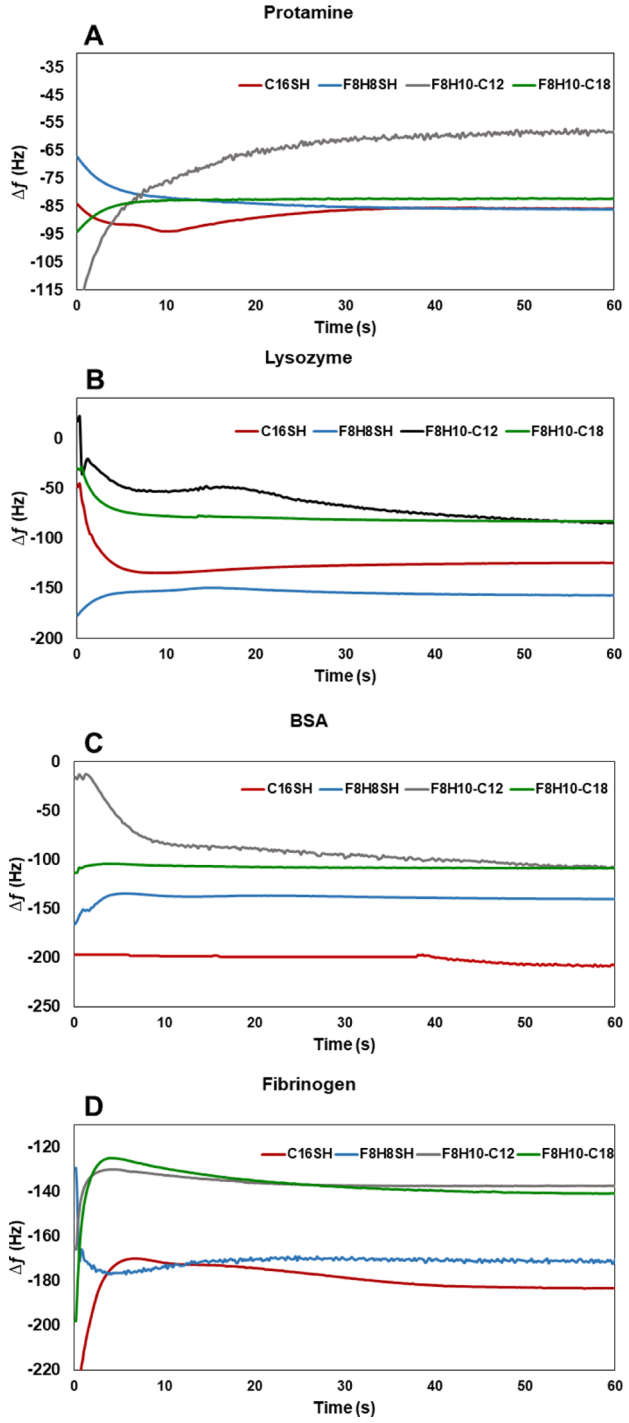

Figure 5. Change in frequency *vs* time for SAMs derived from **C16SH**, **F8H8SH**, **F8H10-C12**, and **F8H10-C18** after 1 h exposure to 1 mg/mL of protein in PBS solution: (A) protamine, (B) lysosome, (C) BSA, and (D) fibrinogen.

https://dx.doi.org/10.1021/acsabm.0c01409
ACS Appl. Bio Mater. 2021, 4, 1563−1572

Table 4. Protein Mass Loading on SAMs Derived from C16SH, F8H8SH, F8H8-C12, and F8H8-C18 after 1 h Exposure to 1 mg/mL of Protein in PBS[a]

SAM	protein loading—ng/cm^2			
	protamine	lysozyme	BSA	fibrinogen
C16SH	392 ± 23	541 ± 89	789 ± 64	792 ± 10
F8H8SH	369 ± 150	671 ± 31	618 ± 76	793 ± 54
F8H10-C12	253 ± 69	406 ± 64	410 ± 53	571 ± 50
F8H10-C18	353 ± 25	410 ± 21	458 ± 19	565 ± 61

[a]Values were calculated from QCM data obtained as described in the Supporting Information.

observed for the **F8H10-C18** SAMs can be attributed to unfavorable interactions between the two phase-incompatible hydrocarbon and fluorocarbon tail groups that give rise to a loosely packed mixture of chains that expose both CH_2 and CF_2 groups—mixtures that are not found in nature and can plausibly lead to diminished protein adsorption.

The QCM data in Figure 5 and Table 4 also offer no convincing evidence that the size/molecular weight of the proteins, the net charge of the proteins, or the surface energies of the SAMs influence protein adsorption in a systematic manner. These data provide further support for our hypothesis that when comparing the respective proteins, the relative degree of protein adsorption is predominantly influenced by the sticky nature of the respective proteins,[49,50] exhibiting the greatest degree of adsorption on the low surface energy SAMs.

Ellipsometric Thickness Measurements. The ellipsometric thicknesses for all SAMs examined are provided in Table S1 in the Supporting Information, where the data confirm monolayer formation and are consistent with literature values.[39,40] Figure 3C graphically presents the changes in thickness after protein exposure, and Table 5 lists the

Table 5. Change in Ellipsometric Thickness Values of the SAMs after Exposure to 1 mg/mL of Protein Solution in PBS

SAM	thickness (Å)			
	protamine	lysozyme	BSA	fibrinogen
C16SH	3 ± 1	21 ± 4	21 ± 6	37 ± 3
F8H8SH	4 ± 2	23 ± 3	17 ± 1	45 ± 11
F8H10-C12	7 ± 1	19 ± 1	21 ± 2	27 ± 2
F8H10-C18	3 ± 2	22 ± 6	16 ± 5	30 ± 5

numerical thickness values. As noted above, the adsorption data for fibrinogen are consistent with the trends observed by SPR and QCM, namely, the SAMs generated from bidentate **F8H10-C12** and **F8H10-C18** were more resistant to the adsorption of fibrinogen than the SAMs generated from monodentate **C16SH** and **F8H8SH**. This trend was not evident in the adsorption behaviors of protamine, BSA, and lysozyme on the SAMs as evaluated by ellipsometry. Specifically, the ellipsometric thicknesses upon protein exposure were largely within the experimental error on all SAMs for each protein examined, save for fibrinogen (see Table 5). These unanticipated results lead us to caution the sole use of ellipsometric measurements to evaluate the antifouling properties of interfaces.

CONCLUSIONS

The protein-resistant properties of SAMs generated from partially fluorinated spiroalkanedithiols, **F8H10-C12** and **F8H10-C18**, and their monodentate analogues **C16SH** and **F8H8SH** were measured using SPR, QCM, and ellipsometry. Proteins having a wide range of physical properties were used to provide a holistic understanding of protein resistance on the SAMs. The studies found that biofilms are less prone to form on the mixed hydrocarbon/fluorocarbon-terminated bidentate SAMs derived from **F8H10-C12** and **F8H10-C18** than on the single-component monodentate SAMs derived from **C16SH** and **F8H8SH**. The enhanced protein resistance observed for the **F8H10-C12** SAMs was attributed to the extension of the hydrophobic helical **F8** fluorinated chains above the underlying densely packed alkyl chains, thereby exposing greater numbers of antiadhesive interfacial CF_2 groups per unit area than in the **F8H8SH** SAMs. Similarly, the enhanced protein resistance observed for the **F8H10-C18** SAMs was attributed to unfavorable interactions between the two phase-incompatible hydrocarbon and fluorocarbon tail groups which give rise to a loosely packed mixture of "conflicted" chains that expose both CH_2 and CF_2 groups—mixtures that are not found in nature and can plausibly lead to diminished protein adsorption. While the SPR and QCM data provided no convincing evidence that the size/molecular weight of the proteins, the net charge of the proteins, or the surface energies of the SAMs influence protein adsorption in a systematic manner, these results are consistent with a model in which the relative degree of protein adsorption on these low surface energy interfaces is predominantly influenced by the sticky nature of the respective proteins.[49,50] The studies also found that the SPR and QCM measurements in most cases were able to distinguish the adsorption trends for the SAMs and proteins examined, but the ellipsometric thickness measurements were less discriminating. The experiments presented herein encompass typical standards for the evaluation of biofilm formation in anticipation of future applications of these model surface coatings and polymeric analogues to follow. Potential substrates include systems ranging from medical implants to oil pipelines and marine-based machines and structures.

ASSOCIATED CONTENT

Supporting Information

The Supporting Information is available free of charge at https://pubs.acs.org/doi/10.1021/acsabm.0c01409.

Details of the materials and experimental methods, ellipsometric thickness values for the untreated SAMs, and details of the surface energy calculations including numerical values provided (PDF)

AUTHOR INFORMATION

Corresponding Author

T. Randall Lee − *Department of Chemistry and the Texas Center for Superconductivity, University of Houston, Houston, Texas 77204-5003, United States;* orcid.org/0000-0001-9584-8861; Email: trlee@uh.edu

Authors

Lydia R. St. Hill − *Department of Chemistry and the Texas Center for Superconductivity, University of Houston, Houston, Texas 77204-5003, United States*

https://dx.doi.org/10.1021/acsabm.0c01409
ACS Appl. Bio Mater. 2021, 4, 1563−1572

John W. Craft, Jr − *Department of Biology and Biochemistry, University of Houston, Houston, Texas 77204-5001, United States*

Pawilai Chinwangso − *Department of Chemistry and the Texas Center for Superconductivity, University of Houston, Houston, Texas 77204-5003, United States*

Hung-Vu Tran − *Department of Chemistry and the Texas Center for Superconductivity, University of Houston, Houston, Texas 77204-5003, United States;* orcid.org/0000-0001-8536-2737

Maria D. Marquez − *Department of Chemistry and the Texas Center for Superconductivity, University of Houston, Houston, Texas 77204-5003, United States*

Complete contact information is available at: https://pubs.acs.org/10.1021/acsabm.0c01409

Notes

The authors declare no competing financial interest.

■ ACKNOWLEDGMENTS

The authors are grateful for financial support from the National Science Foundation (CHE-1710561), the Robert A. Welch Foundation (grant no. E-1320), and the Texas Center for Superconductivity at the University of Houston.

■ REFERENCES

(1) Gu, Y.; Yu, L.; Mou, J.; Wu, D.; Xu, M.; Zhou, P.; Ren, Y. Research Strategies to Develop Environmentally Friendly Marine Antifouling Coatings. *Mar. Drugs* **2020**, *18*, 371.

(2) Banerjee, I.; Pangule, R. C.; Kane, R. S. Antifouling Coatings: Recent Developments in the Design of Surfaces That Prevent Fouling by Proteins, Bacteria, and Marine Organisms. *Adv. Mater.* **2011**, *23*, 690−718.

(3) Wang, Z.; Scheres, L.; Xia, H.; Zuilhof, H. Developments and Challenges in Self-Healing Antifouling Materials. *Adv. Funct. Mater.* **2020**, *30*, 1908098.

(4) Huang, C.-J. Advanced Surface Modification Technologies for Biosensors. *Chemical, Gas, and Biosensors for Internet of Things and Related Applications*; Elsevier, 2019; pp 65−86.

(5) Jiang, C.; Wang, G.; Hein, R.; Liu, N.; Luo, X.; Davis, J. J. Antifouling Strategies for Selective in Vitro and in Vivo Sensing. *Chem. Rev.* **2020**, *120*, 3852−3889.

(6) Schlenoff, J. B. Zwitteration: Coating Surfaces with Zwitterionic Functionality to Reduce Nonspecific Adsorption. *Langmuir* **2014**, *30*, 9625−9636.

(7) Bacha, A.; Méghabar, R. Development of Coatings Marine Antifouling Based on Perfluorinated Surfactants Synthesis and Physicochemical Study. *J. Surf. Eng. Mater. Adv. Technol.* **2014**, *04*, 87−97.

(8) Huang, C.-J.; Zheng, Y.-Y. Controlled Silanization Using Functional Silatrane for Thin and Homogeneous Antifouling Coatings. *Langmuir* **2019**, *35*, 1662−1671.

(9) Xie, C.; Guo, H.; Zhao, W.; Zhang, L. Environmentally Friendly Marine Antifouling Coating Based on a Synergistic Strategy. *Langmuir* **2020**, *36*, 2396−2402.

(10) Badv, M.; Imani, S. M.; Weitz, J. I.; Didar, T. F. Lubricant-Infused Surfaces with Built-In Functional Biomolecules Exhibit Simultaneous Repellency and Tunable Cell Adhesion. *ACS Nano* **2018**, *12*, 10890−10902.

(11) Lundberg, P.; Bruin, A.; Klijnstra, J. W.; Nyström, A. M.; Johansson, M.; Malkoch, M.; Hult, A. Poly(ethylene glycol)-Based Thiol-ene Hydrogel Coatings−Curing Chemistry, Aqueous Stability, and Potential Marine Antifouling Applications. *ACS Appl. Mater. Interfaces* **2010**, *2*, 903−912.

(12) Prime, K.; Whitesides, G. Self-assembled organic monolayers: model systems for studying adsorption of proteins at surfaces. *Science* **1991**, *252*, 1164−1167.

(13) Estephan, Z. G.; Schlenoff, P. S.; Schlenoff, J. B. Zwitteration as an Alternative to PEGylation. *Langmuir* **2011**, *27*, 6794−6800.

(14) Chen, Y.; Luo, S.-C. Synergistic Effects of Ions and Surface Potentials on Antifouling Poly(3,4-Ethylenedioxythiophene): Comparison of Oligo(Ethylene Glycol) and Phosphorylcholine. *Langmuir* **2019**, *35*, 1199−1210.

(15) Li, L.; Chen, S.; Jiang, S. Protein Interactions with Oligo(Ethylene Glycol) (OEG) Self-Assembled Monolayers: OEG Stability, Surface Packing Density and Protein Adsorption. *J. Biomater. Sci., Polym. Ed.* **2007**, *18*, 1415−1427.

(16) Zenasni, O.; Jamison, A. C.; Lee, T. R. The Impact of Fluorination on the Structure and Properties of Self-Assembled Monolayer Films. *Soft Matter* **2013**, *9*, 6356.

(17) Zenasni, O.; Marquez, M. D.; Jamison, A. C.; Lee, H. J.; Czader, A.; Lee, T. R. Inverted Surface Dipoles in Fluorinated Self-Assembled Monolayers. *Chem. Mater.* **2015**, *27*, 7433−7446.

(18) Rodriguez, D.; Marquez, M. D.; Zenasni, O.; Han, L. T.; Baldelli, S.; Lee, T. R. Surface Dipoles Induce Uniform Orientation in Contacting Polar Liquids. *Chem. Mater.* **2020**, *32*, 7832−7841.

(19) Lee, S.; Park, J.-S.; Lee, T. R. The Wettability of Fluoropolymer Surfaces: Influence of Surface Dipoles. *Langmuir* **2008**, *24*, 4817−4826.

(20) Pujari, S. P.; Spruijt, E.; Cohen Stuart, M. A.; Van Rijn, C. J. M.; Paulusse, J. M. J.; Zuilhof, H. Ultralow Adhesion and Friction of Fluoro-Hydro Alkyne-Derived Self-Assembled Monolayers on H-Terminated Si(111). *Langmuir* **2012**, *28*, 17690−17700.

(21) Colorado, R.; Lee, T. R. Physical Organic Probes of Interfacial Wettability Reveal the Importance of Surface Dipole Effects. *J. Phys. Org. Chem.* **2000**, *13*, 796−807.

(22) Pensa, E.; Cortés, E.; Corthey, G.; Carro, P.; Vericat, C.; Fonticelli, M. H.; Benítez, G.; Rubert, A. A.; Salvarezza, R. C. The Chemistry of the Sulfur-Gold Interface: In Search of a Unified Model. *Acc. Chem. Res.* **2012**, *45*, 1183−1192.

(23) Jamison, A. C.; Zhang, S.; Zenasni, O.; Schwartz, D. K.; Lee, T. R. Fibrillar Self-Organization of a Line-Active Partially Fluorinated Thiol within Binary Self-Assembled Monolayers. *Langmuir* **2012**, *28*, 16834−16844.

(24) Park, C. S.; Lee, H. J.; Jamison, A. C.; Lee, T. R. Robust Thick Polymer Brushes Grafted from Gold Surfaces Using Bidentate Thiol-Based Atom-Transfer Radical Polymerization Initiators. *ACS Appl. Mater. Interfaces* **2016**, *8*, 5586−5594.

(25) Love, J. C.; Estroff, L. A.; Kriebel, J. K.; Nuzzo, R. G.; Whitesides, G. M. Self-Assembled Monolayers of Thiolates on Metals as a Form of Nanotechnology. *Chem. Rev.* **2005**, *105*, 1103−1170.

(26) Shon, Y.-S.; Lee, S.; Colorado, R.; Perry, S. S.; Lee, T. R. Spiroalkanedithiol-Based SAMs Reveal Unique Insight into the Wettabilities and Frictional Properties of Organic Thin Films. *J. Am. Chem. Soc.* **2000**, *122*, 7556−7563.

(27) Park, J.-S.; Vo, A. N.; Barriet, D.; Shon, Y.-S.; Lee, T. R. Systematic Control of the Packing Density of Self-Assembled Monolayers Using Bidentate and Tridentate Chelating Alkanethiols. *Langmuir* **2005**, *21*, 2902−2911.

(28) Whitesides, G. M.; Kriebel, J. K.; Love, J. C. Molecular Engineering of Surfaces Using Self-Assembled Monolayers. *Sci. Prog.* **2005**, *88*, 17−48.

(29) Guo, Z.; Meng, S.; Zhong, W.; Du, Q.; Chou, L. L. Self-Assembly of Silanated Poly(Ethylene Glycol) on Silicon and Glass Surfaces for Improved Haemocompatibility. *Appl. Surf. Sci.* **2009**, *255*, 6771−6780.

(30) Chinwangso, P.; Lee, H. J.; Jamison, A. C.; Marquez, M. D.; Park, C. S.; Lee, T. R. Structure, Wettability, and Thermal Stability of Organic Thin-Films on Gold Generated from the Molecular Self-Assembly of Unsymmetrical Oligo(Ethylene Glycol) Spiroalkanedithiols. *Langmuir* **2017**, *33*, 1751−1762.

(31) Wang, Y.-S.; Yau, S.; Chau, L.-K.; Mohamed, A.; Huang, C.-J. Ultra Low Fouling Zwitterionic Polymers with a Biomimetic Adhesive Group. *Langmuir* **2019**, *35*, 1652−1661.
(32) Lee, B. S.; Chi, Y. S.; Lee, K.-B.; Kim, Y.-G.; Choi, I. S. Functionalization of Poly(oligo(ethylene glycol) methacrylate) Films on Gold and Si/SiO2for Immobilization of Proteins and Cells: SPR and QCM Studies. *Biomacromolecules* **2007**, *8*, 3922−3929.
(33) Lee, H.-H.; Gavutis, M.; Ruželė, Ž.; Valiokas, R.; Liedberg, B. Mixed Self-Assembled Monolayers with Terminal Deuterated Anchors: Characterization and Probing of Model Lipid Membrane Formation. *J. Phys. Chem. B* **2018**, *122*, 8201−8210.
(34) Lee, H. J.; Jamison, A. C.; Lee, T. R. Two Are Better than One: Bidentate Adsorbates Offer Precise Control of Interfacial Composition and Properties. *Chem. Mater.* **2016**, *28*, 5356−5364.
(35) Colorado, R.; Lee, T. R. Wettabilities of Self-Assembled Monolayers on Gold Generated from Progressively Fluorinated Alkanethiols. *Langmuir* **2003**, *19*, 3288−3296.
(36) Fukushima, H.; Seki, S.; Nishikawa, T.; Takiguchi, H.; Tamada, K.; Abe, K.; Colorado, R.; Graupe, M.; Shmakova, O. E.; Lee, T. R. Microstructure, Wettability, and Thermal Stability of Semifluorinated Self-Assembled Monolayers (SAMs) on Gold. *J. Phys. Chem. B* **2000**, *104*, 7417−7423.
(37) Yuan, Y.; Yam, C. M.; Shmakova, O. E.; Colorado, R.; Graupe, M.; Fukushima, H.; Moore, H. J.; Lee, T. R. Solution-Phase Desorption of Self-Assembled Monolayers on Gold Derived from Terminally Perfluorinated Alkanethiols. *J. Phys. Chem. C* **2011**, *115*, 19749−19760.
(38) Marquez, M. D.; Zenasni, O.; Jamison, A. C.; Lee, T. R. Homogeneously Mixed Monolayers: Emergence of Compositionally Conflicted Interfaces. *Langmuir* **2017**, *33*, 8839−8855.
(39) Chinwangso, P.; Lee, H. J.; Lee, T. R. Self-Assembled Monolayers Generated from Unsymmetrical Partially Fluorinated Spiroalkanedithiols. *Langmuir* **2015**, *31*, 13341−13349.
(40) Chinwangso, P.; St. Hill, L.; Marquez, M.; Lee, T. Unsymmetrical Spiroalkanedithiols Having Mixed Fluorinated and Alkyl Tailgroups of Varying Length: Film Structure and Interfacial Properties. *Molecules* **2018**, *23*, 2632.
(41) Smith, R. K.; Reed, S. M.; Lewis, P. A.; Monnell, J. D.; Clegg, R. S.; Kelly, K. F.; Bumm, L. A.; Hutchison, J. E.; Weiss, P. S. Phase Separation within a Binary Self-Assembled Monolayer on Au{111} Driven by an Amide-Containing Alkanethiol. *J. Phys. Chem. B* **2001**, *105*, 1119−1122.
(42) Jackson, A. M.; Myerson, J. W.; Stellacci, F. Spontaneous Assembly of Subnanometre-Ordered Domains in the Ligand Shell of Monolayer-Protected Nanoparticles. *Nat. Mater.* **2004**, *3*, 330−336.
(43) Yaliraki, S. N.; Longo, G.; Gale, E.; Szleifer, I.; Ratner, M. A. Stability and Phase Separation in Mixed Self-Assembled Monolayers. *J. Chem. Phys.* **2006**, *125*, 074708.
(44) Fetisov, E. O.; Siepmann, J. I. Structure and Phase Behavior of Mixed Self-Assembled Alkanethiolate Monolayers on Gold Nanoparticles: A Monte Carlo Study. *J. Phys. Chem. B* **2016**, *120*, 1972−1978.
(45) Chinwangso, P.; Jamison, A. C.; Lee, T. R. Multidentate Adsorbates for Self-Assembled Monolayer Films. *Acc. Chem. Res.* **2011**, *44*, 511−519.
(46) Murphy, M. C.; Klein, H. G. *Blood Component and Pharmacologic Therapy for Hemostatic Disorders*, 4th ed.; Elsevier Inc., 2013.
(47) Colvin, J. R. The Size and Shape of Lysozyme. *Can. J. Chem.* **1952**, *30*, 831−834.
(48) Tsai, D.-H.; Delrio, F. W.; Keene, A. M.; Tyner, K. M.; MacCuspie, R. I.; Cho, T. J.; Zachariah, M. R.; Hackley, V. A. Adsorption and Conformation of Serum Albumin Protein on Gold Nanoparticles Investigated Using Dimensional Measurements and in Situ Spectroscopic Methods. *Langmuir* **2011**, *27*, 2464−2477.
(49) Pietrocola, G.; Visai, L.; Valtulina, V.; Vignati, E.; Rindi, S.; Arciola, C. R.; Piazza, R.; Speziale, P. Multiple Interactions of FbsA, a Surface Protein fromStreptococcus agalactiae, with Fibrinogen: Affinity, Stoichiometry, and Structural Characterization†. *Biochemistry* **2006**, *45*, 12840−12852.
(50) Furlan, M. Sticky and Promiscuous Plasma Proteins Maintain the Equilibrium between Bleeding and Thrombosis. *Swiss Med. Wkly.* **2002**, *132*, 181−189.
(51) Marucco, A.; Catalano, F.; Fenoglio, I.; Turci, F.; Martra, G.; Fubini, B. Possible Chemical Source of Discrepancy between in Vitro and in Vivo Tests in Nanotoxicology Caused by Strong Adsorption of Buffer Components. *Chem. Res. Toxicol.* **2015**, *28*, 87−91.
(52) Parkes, M.; Myant, C.; Cann, P. M.; Wong, J. S. S. The Effect of Buffer Solution Choice on Protein Adsorption and Lubrication. *Tribol. Int.* **2014**, *72*, 108−117.
(53) Bakhtiar, R. Surface Plasmon Resonance Spectroscopy: A Versatile Technique in a Biochemist's Toolbox. *J. Chem. Educ.* **2013**, *90*, 203−209.
(54) Holmlin, R. E.; Chen, X.; Chapman, R. G.; Takayama, S.; Whitesides, G. M. Zwitterionic SAMs That Resist Nonspecific Adsorption of Protein from Aqueous Buffer. *Langmuir* **2001**, *17*, 2841−2850.
(55) Lin, P.; Chuang, T.-L.; Chen, P. Z.; Lin, C.-W.; Gu, F. X. Low-Fouling Characteristics of Ultrathin Zwitterionic Cysteine SAMs. *Langmuir* **2019**, *35*, 1756−1767.
(56) Sha, X.; Sun, C.; Xu, X.; Alexander, L.; Loll, P. J.; Penn, L. S. Quartz Crystal Microbalance (QCM): Useful for Developing Procedures for Immobilization of Proteins on Solid Surfaces. *Anal. Chem.* **2012**, *84*, 10298−10305.
(57) Alexander, T. E.; Lozeau, L. D.; Camesano, T. A. QCM-D Characterization of Time-Dependence of Bacterial Adhesion. *Cell Surf.* **2019**, *5*, 100024.
(58) Suthar, J.; Parsons, E. S.; Hoogenboom, B. W.; Williams, G. R.; Guldin, S. Acoustic Immunosensing of Exosomes Using a Quartz Crystal Microbalance with Dissipation Monitoring. *Anal. Chem.* **2020**, *92*, 4082−4093.
(59) Tarnapolsky, A.; Freger, V. Modeling QCM-D Response to Deposition and Attachment of Microparticles and Living Cells. *Anal. Chem.* **2018**, *90*, 13960−13968.
(60) Attwood, S. J.; Kershaw, R.; Uddin, S.; Bishop, S. M.; Welland, M. E. Understanding how charge and hydrophobicity influence globular protein adsorption to alkanethiol and material surfaces. *J. Mater. Chem. B* **2019**, *7*, 2349−2361.
(61) Pflaum, J.; Bracco, G.; Schreiber, F.; Colorado, R.; Shmakova, O. E.; Lee, T. R.; Scoles, G.; Kahn, A. Structure and electronic properties of CH3- and CF3-terminated alkanethiol monolayers on Au(): a scanning tunneling microscopy, surface X-ray and helium scattering study. *Surf. Sci.* **2002**, *498*, 89−104.
(62) Chidsey, C. E. D.; Loiacono, D. N. Chemical Functionality in Self-Assembled Monolayers: Structural and Electrochemical Properties. *Langmuir* **1990**, *6*, 682−691.
(63) Ulman, A.; Eilers, J. E.; Tillman, N. Packing and Molecular Orientation of Alkanethiol Monolayers on Gold Surfaces. *Langmuir* **1989**, *5*, 1147−1152.
(64) Hook, F.; Rodahl, M.; Kasemo, B.; Brzezinski, P. Structural Changes in Hemoglobin during Adsorption to Solid Surfaces: Effects of PH, Ionic Strength, and Ligand Binding. *Proc. Natl. Acad. Sci.* **1998**, *95*, 12271−12276.
(65) Sun, X.; Wu, C.; Hu, J.; Huang, X.; Lu, G.; Feng, C. Antifouling Surfaces Based on Fluorine-Containing Asymmetric Polymer Brushes: Effect of Chain Length of Fluorinated Side Chain. *Langmuir* **2019**, *35*, 1235−1241.
(66) Rickert, J.; Brecht, A.; Göpel, W. Quartz Crystal Microbalances for Quantitative Biosensing and Characterizing Protein Multilayers. *Biosens. Bioelectron.* **1997**, *12*, 567−575.
(67) Levi, M. D.; Daikhin, L.; Aurbach, D.; Presser, V. Quartz Crystal Microbalance with Dissipation Monitoring (EQCM-D) for in-Situ Studies of Electrodes for Supercapacitors and Batteries: A Mini-Review. *Electrochem. Commun.* **2016**, *67*, 16−21.
(68) Ispas, A.; Bund, A. Electrochemical Quartz Crystal Microbalance. *Encyclopedia of Applied Electrochemistry*; Springer: New York, 2014.

https://dx.doi.org/10.1021/acsabm.0c01409
ACS Appl. Bio Mater. 2021, 4, 1563−1572

(69) Smith, A. L. The Quartz Crystal Microbalance. *Handbook of Thermal Analysis and Calorimetry*; Elsevier, 2008; Vol. 5, pp 133−169.

https://dx.doi.org/10.1021/acsabm.0c01409
ACS Appl. Bio Mater. 2021, 4, 1563−1572